
SOLVING INTEGRATED PROCESS PLANNING AND SCHEDULING PROBLEM VIA GRAPH NEURAL NETWORK BASED DEEP REINFORCEMENT LEARNING

Hongpei Li^{1,*} Han Zhang^{1,*} Ziyang He¹ Yunkai Jia² Bo Jiang¹ Xiang Huang²
 Dongdong Ge³

¹Shanghai University of Finance and Economics

²Cardinal Operations

³Shanghai Jiao Tong University

ABSTRACT

The Integrated Process Planning and Scheduling (IPPS) problem combines process route planning and shop scheduling to achieve high efficiency in manufacturing and maximize resource utilization, which is crucial for modern manufacturing systems. Traditional methods using Mixed Integer Linear Programming (MILP) and heuristic algorithms can not well balance solution quality and speed when solving IPPS. In this paper, we propose a novel end-to-end Deep Reinforcement Learning (DRL) method. We model the IPPS problem as a Markov Decision Process (MDP) and employ a Heterogeneous Graph Neural Network (GNN) to capture the complex relationships among operations, machines, and jobs. To optimize the scheduling strategy, we use Proximal Policy Optimization (PPO). Experimental results show that, compared to traditional methods, our approach significantly improves solution efficiency and quality in large-scale IPPS instances, providing superior scheduling strategies for modern intelligent manufacturing systems.

1 Introduction

Deep Reinforcement Learning (DRL) is a popular technique to learn sequential decision-making in complex problems, combining reinforcement learning with deep learning [1], which has achieved successful applications in various areas including robotics, traffic signal control, and recommendation systems. There is a growing interest in applying DRL to NP-hard combinatorial optimization problems (COPs) [2] to find a reasonable good solution within an acceptable time such as the Traveling Salesman Problem (TSP) and scheduling problems such as Job Shop Scheduling (JSP) and Flexible Job Shop Scheduling Problem (FJSP) [3, 4, 5]. Since DRL inherits the fundamental framework of dynamic programming and Markov Decision Process (MDP), it is naturally suitable for solving multi-stage decision problems transformed from COPs.

Inspired by the successful applications mentioned above, we introduce DRL to the Integrated Process Planning and Scheduling (IPPS) problem, a typical NP-hard COP that is crucial for intelligent manufacturing. IPPS combines two of the most important subsystems in manufacturing systems: process planning and shop scheduling, where the former plans the optimal process route under precedence constraints, and the latter schedules machine assignments, sequences of jobs, and start times based on the known process route. Traditionally, these two subsystems execute sequentially. However, performing them separately can lead to bottleneck resources, conflicts in optimization objectives, and unbalanced machine loads [6]. In contrast, IPPS simultaneously optimizes both process routes and scheduling plans under specific constraints and objectives, such as completion time [7]. Therefore, IPPS has become a popular topic in current production research.

IPPS has been widely applied in the automotive, shipbuilding, chemical, metallurgy, and aerospace manufacturing areas [8, 9, 10] which require modern manufacturing systems with efficiently and dynamically responding to rapidly

*These authors contributed equally to this work.

†Correspondence to: Hongpei Li<ishongpeili@gmail.com>, Bojiang<isybojiang@gmail.com>

changing product demands[11]. However, as a typical NP-hard problem, traditional methods for solving IPPS, such as mixed-integer linear programming and heuristic genetic algorithms [12, 13, 14, 15], struggle to quickly adapt to dynamic, real-world environments with unexpected disruptions due to their computational complexity. Therefore, ensuring the efficiency of IPPS solutions has become a challenging issue.

In combinatorial optimization problems similar to IPPS, DRL methods show advantages in efficiency and accuracy. Taking the FJSP as an example, DRL models the scheduling process as an MDP, using neural network models to collect production environment information and output scheduling priorities. [16] use Priority Dispatching Rules (PDRs) derived from expert experience and employ deep Q-networks to solve FJSP end-to-end. To fully exploit the graph structure of FJSP, [17, 18] model the state of FJSP as a heterogeneous graph, combining graph neural networks with attention mechanisms, which perform well on large-scale problems. Unlike heuristic methods, DRL has strong transfer learning capabilities, quickly adapts to new problems, and provides high-quality solutions.

However, current research rarely uses DRL to solve IPPS. The existing DRL methods used for FJSP cannot apply to IPPS directly due to additional complexity in the decision-making and representation of IPPS while simultaneously solving process route selection and resource scheduling. Thus, in this paper, we propose a novel end-to-end DRL method. We model the IPPS problem as an MDP and employ a Heterogeneous Graph Neural Network (HGNN) to capture the complex relationships among operations, machines, and jobs. To optimize the scheduling strategy, we use Proximal Policy Optimization (PPO).

Contributions To the best of our knowledge, this article is the first to apply DRL to solve the IPPS problem. We formulate an equivalent MDP for IPPS by incorporating an empty action to represent waiting at decision points. Presenting the current state as a heterogeneous graph, we use GNN for feature extraction and generate an operation-machine pair to process next by DRL structure.

- **Exploration Efficiency:** We introduce the concept of combination—a set of indispensable operations for finishing the job—into our action space reduction strategy. While the number of combinations is relatively small, ineffective exploration costs associated with multiple production paths are avoided.
- **Stability and Generalization:** Our state transition process prunes completed or infeasible operations and their connections from the heterogeneous graph, reducing noise and focusing on critical scheduling tasks. Moreover, we propose a dense reward function based on estimated completion times, which outperforms a naive sparse reward related to the actual completion time. Together, our model can generalize effectively across various scheduling environments through a stable training process.
- **Competitive Numerical Performance:** Training on small-size problems with no more than 6 jobs, our DRL approach substantially outperforms in large-scale problems, particularly those with more than 16 jobs over 30,000 variables, achieving an improvement of 11.35% compared to OR-Tools.

2 Related Work

2.1 Conventional IPPS Methods

Traditional IPPS solutions include exact methods like MILP and Constraint Programming (CP). [12] developed MILP models for IPPS using network representations, solved with CPLEX. [13] used logic-based benders decomposition to iteratively solve sub-problems, but these approaches struggle with large-scale problems. Consequently, research has shifted towards heuristic methods.

[14] establish a benchmark dataset using a symbiotic evolutionary algorithm. [19] introduce simulated annealing for optimization, improving performance on Kim’s dataset. Other hybrid methods, such as ant colony optimization [20], tabu search [21], variable neighborhood search [15], and harmony search [22], have been applied to IPPS. While faster than exact algorithms, these approaches lack optimality guarantees.

2.2 DRL-based Scheduling Methods

To enhance solution efficiency and quality, DRL has been applied to scheduling problems like FJSP. [16] combined expert-based Priority Dispatching Rules (PDR) with deep Q-Networks for dynamic FJSP, while [23] proposed an end-to-end DRL method using tripartite graphs. However, these approaches overlook graph structures in scheduling problems.

Recent studies incorporate Graph Neural Networks (GNNs) to capture unique graph information in FJSP. [24] used interlaced graphs and DRL to learn high-quality PDR, while [17] modeled FJSP as an MDP with heterogeneous graphs

and attention mechanisms for state representation. [18] utilized multi-strategy generation and PPO with PDR to restrict the action space, achieving strong performance in large-scale instances.

Most related works focus on using DRL for FJSP, but these methods can't be directly applied to IPPS. Improving solving IPPS with DRL remains a crucial research topic.

3 Preliminaries

3.1 Graph-based IPPS Problem

An IPPS instance is defined by a set of n jobs $\mathcal{J} = \{J_1, J_2, \dots, J_n\}$ and a set of m machines $\mathcal{M} = \{M_1, M_2, \dots, M_m\}$. For each job $J_i \in \mathcal{J}$, J_i has a set of operations $\mathcal{O}_i = \{O_{i1}, O_{i2}, \dots, O_{il}\}$, and each operation O_{ij} in \mathcal{O}_i can be processed on machines belonging to a set of machines $\mathcal{M}_{ij} \subseteq \mathcal{M}$. The time machine M_k processes the operation O_{ij} is denoted as $p_{ijk} \in \mathbb{R}^+$. The most common objective function used to minimize an IPPS problem is makespan, which is defined as $\max_{i,j} T_{ij}$ where T_{ij} is the completion time of O_{ij} .

To complete each job $J_i \in \mathcal{J}$, operations in \mathcal{O}_i must follow certain precedence constraints, which can be represented in an AND/OR graph [25]. In an AND/OR graph, each job begins and ends with a starting node and an ending node, and intermediate nodes represent each operation in \mathcal{O}_i (see Figure 1a). The arrows connecting the nodes represent the precedence between them. Arrows with the attribute 'OR' are called OR-links, and the start nodes of OR-links are OR-connectors. An operation path that begins at an OR-link and ends when it merges with other paths is called an OR-link path. When processing jobs, only one path in OR-paths beginning with the same OR-connectors is chosen. For nodes that are not in any OR-path, all of them should be visited. Following the rules above, we define the set of indispensable operations for finishing the job without considering precedence relationships between operations as a combination. $\mathcal{C}_i = \bigcup_h \mathcal{C}_{ih}$ is the set of all possible combinations of J_i .

Remark 1 The definition of a combination is proposed by [12]. We mainly focus on combination without precedence relationships rather than each processing sequence which shows a specific processing order in this paper, because the number of combinations is much less than the processing sequences that can be up to $O(n!)$, and provides an effective exploration space.

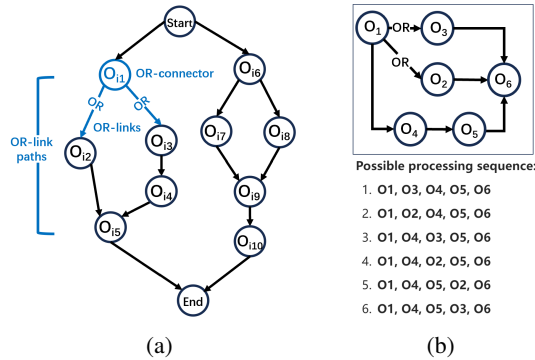


Figure 1: (a) AND/OR graph of an IPPS job. (b) All possible processing sequences for a single instance.

4 Motivation and Novel Ingredient

Motivation: In fact, DRL has been utilized to solve some easier scheduling problems like JSP and FJSP, which however can not be adapted to IPPS. In particular, each job in FJSP has a known single processing sequence, but the processing sequence for each job in IPPS could have $O(n!)$ permutations (see Figure 1b). If we consider all possible sequences in IPPS, then solving one IPPS can be reduced to solving $O(n!)$ FJSP, which becomes computationally infeasible even if DRL for FJSP is fast. Thus directly applying previous DRL methods of FJSP to IPPS is impractical.

Novel Ingredient: In our work, we model IPPS to equivalent MDP formulation, which is proved in Appendix A. While previous works on FJSP could only handle a single sequence, we designed a new heterogeneous graph based on the mentioned AND/OR graph to represent the state in IPPS, incorporating the Combination node category to extract information from the set of processing steps, and we use heterogeneous GNN to extract information and use the

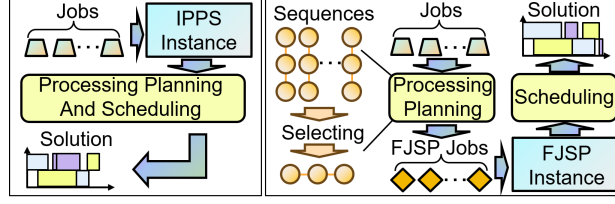


Figure 2: Comparison between IPPS (left) and Processing Planing plus Scheduling (right).

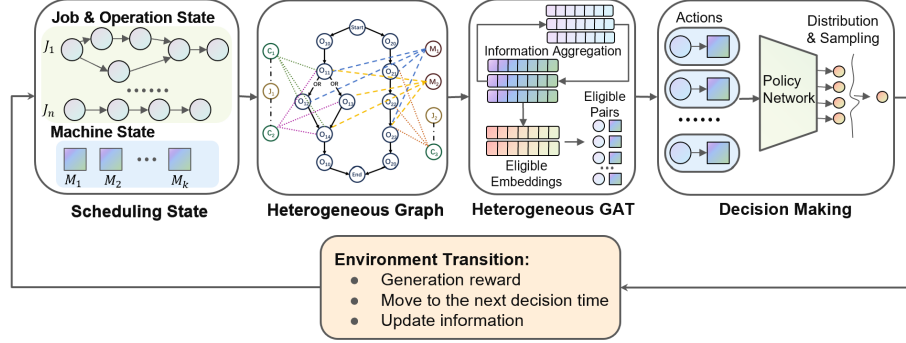


Figure 3: The workflow of the proposed method.

designed model to make decisions. To prevent the ineffective exploration costs caused by multiple production paths, we proposed an action space reduction based on the combination, ensuring that each trajectory selects exactly one processing sequence. Furthermore, we propose a reward function based on the estimated completion time for IPPS, and experiments show that it performs better than the naive reward function.

5 MDP Formulation

To define the Markov Decision Process (MDP) for the IPPS problem, we formulate the state space, action space, state transitions, and reward function as follows. At each decision point, following the completion of an operation, the agent extracts eligible operation-machine pairs based on the current state and decides which pair to perform next.

Notice that all decision points (or time-step) are at an operation’s completion time. Whenever no operation can be processed or we choose to wait until the next time-step, we’ll jump to the next time-step, which is the nearest completion time from the current time. The structure of the heterogeneous graph is illustrated as follows. We will prove the following theorem in Appendix A:

Theorem 1 The introduced MDP formulation is equivalent to the original problem in terms of their optimal solutions.

5.1 State

At each step t , the state s_t represents the status of IPPS problem job completion at the current time t . We formulate the state using a dynamic heterogeneous graph, a directed structure composed of various types of nodes and edges, designed to extract information via GNNs. Previous studies on FJSP [17, 26] usually include three types of nodes in heterogeneous graphs which cannot apply to IPPS problem directly since IPPS additionally requires selecting a combination following the choice of each OR-connector operation. Accordingly, we introduce nodes representing combinations and jobs within our graph to capture information from operations during GNN’s information aggregation, which will be detailed in subsequent sections.

Node types:

- Operations (\mathcal{O}): $O_{ij} \in \mathcal{O}$ denotes the i -th job’s j -th operation.
- Machines (\mathcal{M}): $M_k \in \mathcal{M}$ denotes the k -th machines.
- Combinations (\mathcal{C}): $C_{ih} \in \mathcal{C}$ denote a combination h of job i , which is a set of operations.
- Jobs (\mathcal{J}): $J_i \in \mathcal{J}$ denotes the i -th job.

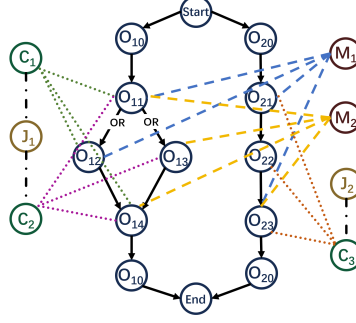


Figure 4: Example of heterogeneous graph.

Edge types:

- $\mathcal{O} \longrightarrow \mathcal{O}$: represent the relationship of prerequisites, which means there is a directed edge from O_{ij} to $O_{ij'}$ if and only if O_{ij} is the last required predecessor operation of $O_{ij'}$.
- $\mathcal{O} \longleftrightarrow \mathcal{C}$: there is an undirected edge between O_{ij} and C_{ih} when $O_{ij} \in C_{ih}$.
- $\mathcal{C} \longleftrightarrow \mathcal{J}$: there is an undirected edge between C_{ih} and J_i when $C_{ih} \subset J_i$.
- $\mathcal{O} \longleftrightarrow \mathcal{M}$: there is an undirected edge between O_{ij} and M_k when M_k can process O_{ij} .

The details of the features in the graph are shown in Appendix B. Figure 4 is a heterogeneous graph of a simple IPPS problem (or initial state). Note that the "start" and "end" points are for representation purposes only, and the nodes marked O_{t0} are supernodes representing where the job J_i begins and ends with 0 processing time for all machines.

5.2 Action Space

In this paper, an action a_t is defined as a feasible operation-machine pair (O-M pair), which means selecting an operation and a machine to process it. However, with numerous ineligible actions, there is a high cost to the agent's exploration. Therefore, we use two action space reduction strategies.

Strategy I: The first strategy to reduce the action space is detecting feasibility, similar to previous FJSP works, such as [17] and [27]. Specifically, candidates during the decision phase are restricted to O-M pairs that involve feasible operations and relevant idle machines, where feasible operations are those that have not been scheduled and all immediate prerequisite tasks have been completed.

Strategy II: The IPPS problem has a more complex structure in which each job's production line is a directed acyclic graph. As described before, we conclude each job with several combinations, and it's evident that the number of combinations that might be chosen in the future, which we call "eligible", is non-increasing during dispatching. Inspired by this, our second reduction strategy is based on detecting eligible combinations. In more detail, we maintain C_t^* , which is a set of eligible combinations. When one of the branches in the OR-connector is selected, all combinations containing other branches in this OR-connector will be removed from C_t^* , and we will only consider operations that belong to at least one combination in C^* . Figure 5 is a simple example that illustrates this strategy.

Above all, at time step t , the action space \mathcal{A}_t is defined as: $\{waiting\} \cup \{(O_{ij}, M_k) | O_{ij} \in (\bigcup_p \{C_t^*\}_p) \cap R_t, M_k \in I_t \cap P_{ij}\}$, where $\{C_t^*\}_p$ is the p -th component of C_t^* (set of eligible combinations), R_t is the set of feasible operations, I_t is the set of idle machines at t , and P_{ij} is the set of machines that can process O_{ij} .

5.3 State Transitions

In each time step, the heterogeneous graph is updated according to the following rules:

- Update the features in the graph as described previously.
- Delete the finished operation nodes along with all arcs connected to these deleted operation nodes.
- When a branch in an OR-connector is selected, delete the combination nodes and operation nodes according to the rule described in "action space reduction", as well as all arcs connected to these deleted nodes.
- Delete machine nodes and job nodes that are no longer connected with any arcs.

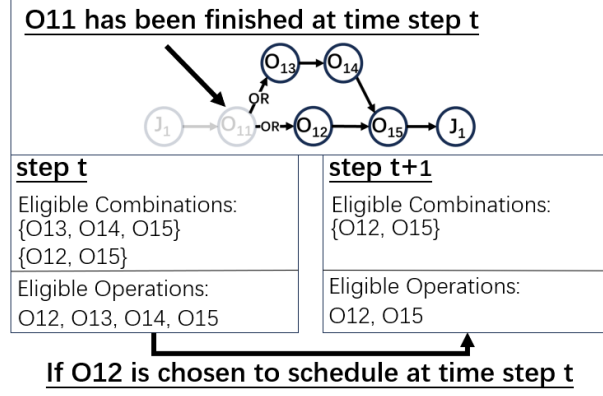


Figure 5: Example of action space reduction strategy II.

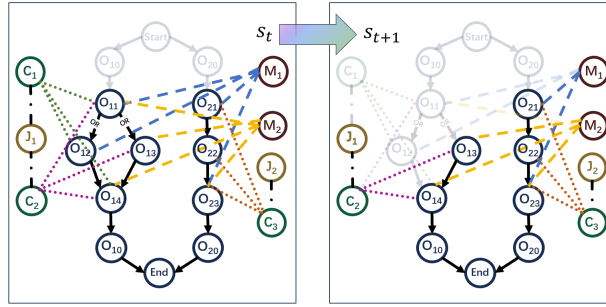
Figure 6: Example of state transition from time-step t to $t + 1$.

Figure 6 illustrates a simple example of state transitions. At time step t , O_{11} is scheduled but not yet completed, and M_1 begins processing O_{12} . Before $t + 1$, no O-M pair is selected because the only feasible operation, O_{21} , can only be processed by M_1 , which is busy processing O_{11} . Once O_{11} is completed, the corresponding node O_{11} and its related arcs are deleted. Post O_{11} 's completion, O_{12} and O_{13} become feasible, and M_1 becomes idle. At $t + 1$, M_1 is assigned to process O_{13} , rendering C_1 ineligible. Consequently, O_{12} and its related arcs are deleted. The features are updated accordingly. Note that super nodes do not impact the process as they finish immediately after being scheduled.

5.4 Reward

The reward function is critical in the MDP, guiding the agent by providing feedback on the effectiveness of the current policy.

Naive Reward: Initially, we define a naive reward function $r_0(s_t, a_t, s_{t+1}) = T(s_t) - T(s_{t+1})$, which represents the change in the actual completion time of the partial schedule. The cumulative naive reward without discount corresponds to the negative makespan. However, due to the significant variation among different IPPS problems, this type of cumulative reward fluctuates greatly, making it difficult to assess the current policy's performance.

Suggested Reward: To address this issue, we propose several advanced reward functions designed to evaluate policies based on relative improvement rather than absolute makespan. For initialization, we set the estimated processing time of each operation as $\hat{p}_{ij} = \min_{k \in P_{ij}} p_{ijk}$ or $\sum_{k \in P_{ij}} p_{ijk} / \|P_{ij}\|$, and aggregate these times by combinations to estimate their ending times \hat{T}_{ih} . We then set $\hat{T}_i = \min_{h \in J_i} \hat{T}_{ih}$ or $\sum_{h \in J_i} \hat{T}_{ih} / \|J_i\|$ as the estimated ending time of jobs and $\hat{T} = \max_i \hat{T}_i$ or $\sum_{i \in J_t^*} \hat{T}_i / \|J_t^*\|$ as the estimated ending time of the entire problem, where J_t^* denotes jobs unfinished at t . At each step, we update the estimated ending times of combinations and the problem using the real processing time and record the changes in estimated ending time as the reward $r(s_t, a_t, s_{t+1}) = \hat{T}(s_t) - \hat{T}(s_{t+1})$. Our experiments demonstrate the effectiveness of this approach; see Appendix F.

5.5 Policy

The policy maps the state space to a probability distribution over the action space. For a given state s , the policy $\pi(s)$ provides the probabilities of the possible actions a in that state.

Mathematically, it can be expressed as: $\pi : \mathcal{S} \rightarrow \mathcal{P}(\mathcal{A})$ where \mathcal{S} is the state space, $\mathcal{P}(\mathcal{A})$ is the probability distribution over the action space \mathcal{A} . We'll detail the policy design later.

6 Neural Networks and Decision Making

In this section, we introduce the method we use for feature extraction and algorithm for policy generation.

6.1 Graph Representation

DRL utilizes neural networks to extract state information. The states in our work are structured and have a variant number of nodes and edges, which cannot be represented as fixed-shaped tensors. Thus, we use graph neural networks (GNNs), which are shown to have higher performance in multiple fields with structured features, such as Combinatorial Optimization (CO) [28, 29] and the recommendation system [30]. One of the most popular and effective GNNs is graph attention networks (GATs), we apply GATv2 [31] here, a modified version of GAT that shows higher efficiency in multiple fields. GATv2 is an aggregation-based GNN that uses dynamic attention mechanisms to aggregate information from neighbors connected by edges. The attention score α_{ij} is calculated as:

$$\alpha_{i,j} = \frac{\exp(e_{ij})}{\sum_{k \in \mathcal{N}(i) \cup \{i\}} \exp(e_{ik})}, \text{ where}$$

$$e_{ij} = \begin{cases} \mathbf{a}^\top \text{LeakyReLU}(\Theta_s \mathbf{x}_i + \Theta_t \mathbf{x}_j), & \text{if no edge features} \\ \mathbf{a}^\top \text{LeakyReLU}(\Theta_s \mathbf{x}_i + \Theta_t \mathbf{x}_j + \Theta_e e_{ij}), & \text{else} \end{cases}$$

The new feature vector for node i is calculated as :

$$\mathbf{x}'_i = \sum_{j \in \mathcal{N}(i) \cup \{i\}} \alpha_{i,j} \Theta_t \mathbf{x}_j$$

where $\mathcal{N}(i)$ is a set of the first-hop neighbors of node i , \mathbf{x}_i is input features (embedding) of node i and \mathbf{x}'_i is output embedding, $\Theta_s, \Theta_t, \Theta_e$ are independent linear transformations for features of start point, features of endpoint and edge features respectively. In our work, we use GATv2 in the heterogeneous graph by doing the aggregation steps described above for each edge type independently (the parameters are also independent) to extract embeddings, which we call HGAT.

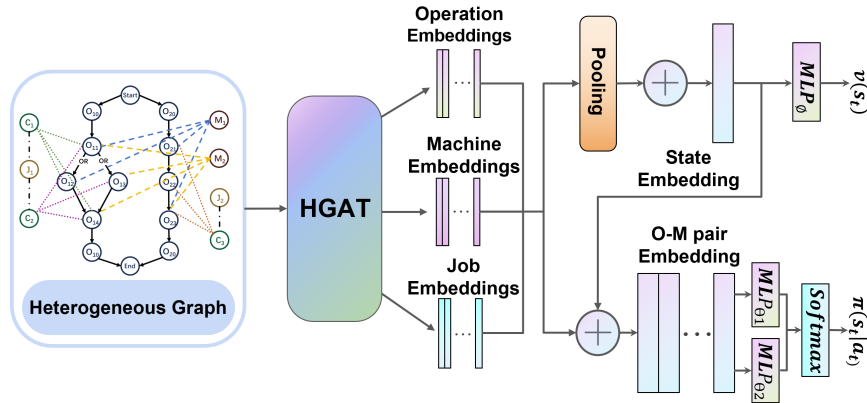


Figure 7: Architecture of neural network.

6.2 Policy Design

A policy $\pi_\theta(a_t|s_t)$ (or actor) is a mapping from state space \mathcal{S} to probability distribution over action space \mathcal{A}_t . The Proximal Policy Optimization (PPO) algorithm [32] is one of our selected methods to train the agent, which also needs a value network $v_\phi(s_t)$ (or critic). In our framework, the HGAT functions as an encoder, with its parameters being shared between the actor and critic albeit in distinct manners. The whole structure of our neural network is shown in Figure 7.

First, HGAT captures information from the heterogeneous graph and generates node embeddings for each type of nodes: $\mathbf{h}_{\mathbf{O}_{ij}}$, $\mathbf{h}_{\mathbf{J}_i}$, $\mathbf{h}_{\mathbf{M}_k}$. Note that node embeddings of combinations are not used in later steps. Define the set of feasible operations as R_t and F_t is the set of operations that are not scheduled and do not have unscheduled immediate prerequisite operations.

To derive the action probabilities in the actor, let the set of eligible O-M pairs at time-step t be:

$$\mathbf{E} = \{(O_{ij}, M_k) | O_{ij} \in (\bigcup_p \{C_t^*\}_p) \cap R_t, M_k \in I_t \cap P_{ij}\}$$

To evaluate the waiting action, define future eligible O-M pairs as those with feasible operations and relevant machines processing other tasks:

$$\mathbf{E}' = \{(O_{ij}, M_k) | O_{ij} \in (\bigcup_p \{C_t^*\}_p) \cap F_t, M_k \in P_{ij}\}$$

The state embedding is:

$$\mathbf{h}_t = \left[\frac{1}{|\mathcal{O}|} \sum_{ij} \mathbf{h}_{\mathbf{O}_{ij}} \parallel \frac{1}{|\mathcal{M}|} \sum_k \mathbf{h}_{\mathbf{M}_k} \parallel \frac{1}{|\mathcal{J}|} \sum_i \mathbf{h}_{\mathbf{J}_i} \right]$$

Also, we define the embedding of an O-M pair as:

$$\mathcal{H}_{ijk} = [\mathbf{h}_{\mathbf{O}_{ij}} \parallel \mathbf{h}_{\mathbf{M}_k} \parallel \mathbf{h}_{\mathbf{J}_i} \parallel \mathbf{h}_t]$$

The priority γ of each eligible pair $(O_{ij}, M_k) \in \mathbf{E}$ is calculated as:

$$\gamma(a_t|s_t) = \text{MLP}_{\theta_1}(\mathcal{H}_{ijk})$$

and the waiting priority γ is calculated as:

$$\gamma(a_t|s_t) = \sum_{(O_{ij}, M_k) \in \mathbf{E}'} \alpha_{ijk} \text{MLP}_{\theta_2}(\mathcal{H}_{ijk})$$

where the attention score α_{ijk} is calculated as follows:

$$\alpha_{ijk} = \frac{\exp[\text{MLP}_{\theta_1}(\mathcal{H}_{ijk})]}{\sum_{(O_{i'j'}, M_{k'}) \in \mathbf{E}'} \exp[\text{MLP}_{\theta_1}(\mathcal{H}_{i'j'k'})]}$$

It should be noted that the independent parameters θ_1 and θ_2 are utilized to process eligible pairs and waiting actions, respectively. In addition, θ_1 is used to determine the weighting of each future eligible pair for the priority of waiting. This is because the importance of each future eligible pair varies, and MLP_{θ_1} can be used to assess the importance of each eligible pair, which in turn informs the weighting of future eligible pairs when calculating the priority of waiting actions.

The probabilities for each action a_t are calculated by a softmax layer over priorities, which is actually the actor $\pi_\theta(a_t|s_t)$:

$$\pi_\theta(a_t|s_t) = \frac{\exp[\gamma(a_t|s_t)]}{\sum_{a'_t \in \mathcal{A}_t} \exp[\gamma(a'_t|s_t)]}$$

The critic $v_\phi(s_t)$ is derived from the state embedding using a MLP:

$$v_\phi(s_t) = \text{MLP}_\phi(\mathbf{h}_t)$$

7 Experiments

7.1 Dataset

To evaluate the efficiency of our method, we conduct 3 experiments on two synthetic datasets of different scales and a public benchmark dataset from [14].

Synthetic Dataset: Based on the structure of AND/OR graph, we generate jobs by computing direct acyclic graphs and add OR-paths recursively. After assigning machines and corresponding processing time to each operation under a certain distribution, we randomly combine jobs for various IPPS problems. For details, refer to Appendix D.

Public Dataset: A widely recognized benchmark in IPPS research introduced by [14]. Kim dataset contains 24 instances with different flexibility.

7.2 Implementation Details

Let N_1, N_2, N_3 be the number of training, validation and testing instances, and $m \times n$ denotes the problem size where m and n are the number of jobs and machines, respectively. Training instances are generated from 1000 jobs with corresponding machine numbers, which actually consist of $N_1 = \binom{1000}{\text{job number}}$ problems. We train three models, each based on synthetic datasets of different problem sizes: 4×5 , 5×3 , and 6×5 , which are all relatively small yet complicated and have a validation size of $N_2 = 20$.

In Experiment 1, we evaluate the models on symmetric datasets that draw on the same size and distribution as the training set. To assess the generalization performance of the trained policies, Experiments 2 and 3 are conducted on a public dataset and on large-scale generated datasets with sizes 16×20 and 20×25 , respectively. In all experiments, the size of all test sets is $N_3 = 50$, and we use DRL-G (only choose actions with the highest probability) and DRL-S (choose actions according to the probability distribution) to evaluate policy performance. For details on infrastructure and configurations, please refer to Appendix E.

7.3 Baseline

We compare our model with two types of baseline algorithms.

- **OR-Tools:** OR-Tools is an open source toolbox by Google [33], which includes the CP-SAT solver, a powerful constraint programming solver known for its strong performance in industrial scheduling [34]. In this paper, we use the CP-SAT solver to implement the MILP model, which is shown in Appendix C, from [12] to obtain exact solutions in 1800 seconds (3600s for Experiment 3).
- **Greedy:** Dispatching rules have shown significant potential in IPPS problems [35]. We select rules for operation sequencing and machine assignment, respectively. For operation selection, we use rules including Most Work Remaining (MWKR), Most Operations Remaining (MOR), First In First Out (FIFO), and probability described in [35]. Machine assignment is based on the priority calculated from the Shortest Processing Time (SPT), Earliest Finish Time (EFT), and Least Utilized Machine (LUM). In each problem, we randomly choose a combination for each job, reducing a complex IPPS problem to a simplified FJSP problem. Then, at each step, the next operation and the corresponding machine are determined by their rank under certain dispatching rules. Details are attached in Appendix G.

7.4 Evaluation

In order to compare method performance from both efficiency and quality, we use Makespan, Gap, and Time as evaluation metrics, where Makespan refers to the average final optimization objective, Gap is the average relative difference compared to Makespan of OR-Tools, and Time measures the average computation time. For the DRL-Sampling method, we run each instance 50 times and select the best value as the final result. For greedy algorithms, we choose the result of the best priority dispatching rules for each whole dataset.

7.5 Results and Analysis

As shown in Table 1, in all training sizes, Experiment 1 demonstrates that our model consistently outperforms the Greedy method in terms of solution quality, while also being faster than all baseline methods. Our method consistently achieves a smaller gap in relation to OR-Tools compared to the Greedy method, with reductions ranging from 3% to 25%, highlighting the effectiveness of our approach.

Table 1: Evaluation on instances of training sizes.

	Size	OR-Tools	DRL-G	DRL-S	Best Greedy
4×5	Makespan	389.99	423.6	403.19	429.73
	Gap [†]	-	7.43%	2.92%	8.79%
	Time (s)	1769.31	7.65	10.23(0.20) [*]	91.01(1.82) [*]
5×3	Makespan	452.36	505.2	474.44	590.76
	Gap [†]	-	11.68%	4.88%	30.60%
	Time (s)	1789.79	7.90	15.54(0.31)	48.45(0.97)
6×5	Makespan	442.14	487.94	462.04	506.63
	Gap [†]	-	10.36%	4.50%	14.59%
	Time (s)	1798.84	8.37	14.68(0.29)	139.76(2.80)

^{*} The value in parentheses is the time for a single epoch. We ran multiple times and selected the Makespan.

[†] Gap is relative to OR-Tools.

Table 2: Performance on the Public Benchmark Kim dataset.

Dataset		Kim		
		Makespan	Gap [†]	Time(s)
LB[*]		387.93	-	-
	OR-Tools	392.08	1.07%	1796.37
DRL-G	4×5	445.17	14.76%	11.94
	5×3	451.33	16.34%	17.79
	6×5	444.25	14.52%	12.12
DRL-S	4×5	416.42	7.34%	23.31(0.97)
	5×3	417	7.49%	34.32(0.67)
	6×5	416.21	7.29%	23.87(0.48)
Best Greedy		458.38	18.16%	82.24(1.64)

^{*} LB indicates the lower bound on the makespan.

[†] Gap is relative to the OR-Tools makespan.

Applying our model to the public dataset, the result of Experiment 2 in Table 2 shows similar advantages as Experiment 2, reflecting the generalization capability of our approach. Moreover, as shown by the detailed results of Kim dataset in Appendix H, our advantages get larger as the problem size increases.

Experiment 3 (see Table 3) further confirms our advantages in large-scale problems. Although OR-Tools cannot even find a feasible solution, the solving time of DRL is less than one minute. Also, DRL outperforms than OR-Tools in OR-Tools-feasible problems up to 11.35%. Strongly proving patterns learned in small and medium instances remain effective in solving larger problems.

Due to page limitations, please refer to Appendix F for more numerical experiments.

8 Conclusions

The IPPS problem is a critical challenge in combinatorial optimization in modern manufacturing systems. In this paper, we propose a novel DRL approach to solving IPPS, which results in a reduced exploration state space, faster solving speed, and smaller makespan gaps compared to greedy algorithms. Extensive experiments on synthetic and benchmark datasets demonstrate the efficiency of our method, particularly in large-scale problems.

Table 3: Generalization performance on large-sized instances.

Dataset	Method	Makespan		Gap [‡]	Time(s)	
		Feasible [*]	All [†]			
16×20	OR-Tools		566.07	-	1800 (7/50 time out)	
	DRL-G	4×5	538.37	537.84	-4.89%	19.77
		5×3	543.17	542.22	-4.05%	32.67
		6×5	542.2	539.54	-4.22%	21.89
	DRL-S	4×5	518.22	527.06	-8.45%	40.59(0.81)
		5×3	517.07	515.48	-8.66%	65.15(1.30)
		6×5	518.63	517.06	-8.38%	41.00(0.82)
	Best Greedy		544.80	544.89	-3.76%	148.66(2.97)
	20×25	OR-Tools		547.03	-	3600 (16/50 time out)
		DRL-G	4×5	508.85	518.28	-7.00%
5×3			510.94	519.86	-6.60%	42.37
6×5			512.00	519.10	-6.40%	28.23
DRL-S		4×5	484.97	495.26	-11.35%	56.34(1.13)
		5×3	486.15	496.84	-11.13%	87.25(1.75)
		6×5	485.67	495.24	-11.21%	56.88(1.14)
Best Greedy			513.83	524.09	-6.10%	186.42(3.73)

^{*} Problem set that is feasible to OR-Tools.

[‡] Gap is relative to OR-Tools.

References

- [1] Ashish Kumar Shakya, Gopinatha Pillai, and Sohom Chakrabarty. Reinforcement learning algorithms: A brief survey. *Expert Systems with Applications*, 231:120495, 2023.
- [2] Quentin Cappart, Thierry Moisan, Louis-Martin Rousseau, Isabeau Prémont-Schwarz, and Andre A Cire. Combining reinforcement learning and constraint programming for combinatorial optimization. In *Proceedings of the AAAI Conference on Artificial Intelligence*, volume 35, pages 3677–3687, 2021.
- [3] Rongkai Zhang, Anatolii Prokhorchuk, and Justin Dauwels. Deep reinforcement learning for traveling salesman problem with time windows and rejections. In *2020 International Joint Conference on Neural Networks (IJCNN)*, pages 1–8. IEEE, 2020.
- [4] J.D. Zhang, Z. He, W.H. Chan, and C.Y. Chow. Deepmag: Deep reinforcement learning with multi-agent graphs for flexible job shop scheduling. *Knowledge-Based Systems*, 259:110083, 2023.
- [5] Y. Liu, X. Zuo, G. Ai, and Y. Liu. A reinforcement learning-based approach for online bus scheduling. *Knowledge-Based Systems*, 271:110584, 2023.
- [6] Qihao Liu, Xinyu Li, Liang Gao, and Guangchen Wang. Mathematical model and discrete artificial bee colony algorithm for distributed integrated process planning and scheduling. *Journal of Manufacturing Systems*, 61:300–310, 2021.
- [7] Rakesh Kumar Phanden, Ajai Jain, and J. Paulo Davim, editors. *Integration of Process Planning and Scheduling Approaches and Algorithms*. Elsevier, 2021.
- [8] Gang Du Yujie Ma and Yingying Zhang. Dynamic hierarchical collaborative optimisation for process planning and scheduling using crowdsourcing strategies. *International Journal of Production Research*, 60(8):2404–2424, 2022.
- [9] Premaratne Samaranayake and Sampath Kiridena. Aircraft maintenance planning and scheduling: an integrated framework. *Journal of Quality in Maintenance Engineering*, 18(4):432–453, 2012.
- [10] Maria LR Varela, Goran D Putnik, Vijay K Manupati, Gadhamsetty Rajyalakshmi, Justyna Trojanowska, and José Machado. Integrated process planning and scheduling in networked manufacturing systems for i4. 0: a review and framework proposal. *Wireless Networks*, 27:1587–1599, 2021.
- [11] J. Zhou, Y. Zhou, B. Wang, and J. Zang. Human-cyber-physical systems (hcpss) in the context of new-generation intelligent manufacturing. *Engineering*, 5(4):624–636, 2019.

- [12] Liangliang Jin, Qiuhua Tang, Chaoyong Zhang, Xinyu Shao, and Guangdong Tian. More milp models for integrated process planning and scheduling. *International Journal of Production Research*, 54:4387 – 4402, 2016.
- [13] R. Barzanji, B. Naderi, and M. A. Begen. Decomposition algorithms for the integrated process planning and scheduling problem. *Omega*, 93, 2020.
- [14] Y. K. Kim, K. Park, and J. Ko. A symbiotic evolutionary algorithm for the integration of process planning and job shop scheduling. *Computers & Operations Research*, 30(8):1151–1171, 2003.
- [15] Y. Li, L. Gao, Q. K. Pan, L. Wan, and K.-M. Chao. An effective hybrid genetic algorithm and variable neighborhood search for integrated process planning and scheduling in a packaging machine workshop. *IEEE Transactions on Systems, Man, and Cybernetics: Systems*, 49(10):1933–1945, 2018.
- [16] S. Luo, L. Zhang, and Y. Fan. Dynamic multi-objective scheduling for flexible job shop by deep reinforcement learning. *Computers & Industrial Engineering*, 159:107489, 2021.
- [17] Wen Song, Xinyang Chen, Qiqiang Li, and Zhiguang Cao. Flexible job-shop scheduling via graph neural network and deep reinforcement learning. *IEEE Transactions on Industrial Informatics*, 19(2):1600–1610, 2023.
- [18] I. Echeverria, M. Murua, and R. Santana. Solving the flexible job-shop scheduling problem through an enhanced deep reinforcement learning approach. *arXiv preprint arXiv:*, 2023.
- [19] W. D. Li and C. A. McMahon. A simulated annealing-based optimization approach for integrated process planning and scheduling. *International Journal of Computer Integrated Manufacturing*, 20(1):80–95, 2007.
- [20] C. Leung, T. Wong, K.-L. Mak, and R. Y. Fung. Integrated process planning and scheduling by an agent-based ant colony optimization. *Computers & Industrial Engineering*, 59(1):166–180, 2010.
- [21] X. Li, X. Shao, L. Gao, and W. Qian. An effective hybrid algorithm for integrated process planning and scheduling. *International Journal of Production Economics*, 126(2):289–298, 2010.
- [22] X. Wu and J. Li. Two layered approaches integrating harmony search with genetic algorithm for the integrated process planning and scheduling problem. *Computers & Industrial Engineering*, 2021.
- [23] B. Han and J. Yang. A deep reinforcement learning based solution for flexible job shop scheduling problem. *International Journal of Simulation Modelling*, 20(2):375–386, 2021.
- [24] C. Zhang, W. Song, Z. Cao, J. Zhang, P. S. Tan, and X. Chi. Learning to dispatch for job shop scheduling via deep reinforcement learning. *Advances in Neural Information Processing Systems*, 33, 2020.
- [25] YC Ho and CL Moodie. Solving cell formation problems in a manufacturing environment with flexible processing and routing capabilities. *International Journal of Production Research*, 34(11):2901–2923, 1996.
- [26] Runqing Wang, Gang Wang, Jian Sun, Fang Deng, and Jie Chen. Flexible job shop scheduling via dual attention network based reinforcement learning, 2023.
- [27] I. Echeverria, M. Murua, and R. Santana. Leveraging constraint programming in a deep learning approach for dynamically solving the flexible job-shop scheduling problem. *arXiv preprint arXiv:2403.09249*, 2024.
- [28] Maxime Gasse, Didier Chételat, Nicola Ferroni, Laurent Charlin, and Andrea Lodi. Exact combinatorial optimization with graph convolutional neural networks, 2019.
- [29] Tianhao Liu, Shanwen Pu, Dongdong Ge, and Yinyu Ye. Learning to pivot as a smart expert. *Proceedings of the AAAI Conference on Artificial Intelligence*, 38(8):8073–8081, March 2024.
- [30] Chen Gao, Yu Zheng, Nian Li, Yinfeng Li, Yingrong Qin, Jinghua Piao, Yuhuan Quan, Jianxin Chang, Depeng Jin, Xiangnan He, and Yong Li. A survey of graph neural networks for recommender systems: Challenges, methods, and directions, 2023.
- [31] Shaked Brody, Uri Alon, and Eran Yahav. How attentive are graph attention networks? *ArXiv*, abs/2105.14491, 2021.
- [32] John Schulman, Filip Wolski, Prafulla Dhariwal, Alec Radford, and Oleg Klimov. Proximal policy optimization algorithms. *arXiv preprint arXiv:1707.06347*, 2017.
- [33] Google. Or-tools. <https://github.com/google/or-tools>, 2024. Accessed: 2024-07-30.
- [34] G. Da Col and E. C. Teppan. Industrial size job shop scheduling tackled by present day cp solvers. In *International Conference on Principles and Practice of Constraint Programming*, pages 144–160. Springer, 2019.
- [35] Muhammad Farhan Ausaf, Liang Gao, Xinyu Li, and Ghiath Al Aqel. A priority-based heuristic algorithm (pbha) for optimizing integrated process planning and scheduling problem. *Cogent Engineering*, 2(1):1070494, 2015.

- [36] Adam Paszke, Sam Gross, Francisco Massa, Adam Lerer, James Bradbury, Gregory Chanan, Trevor Killeen, Zeming Lin, Natalia Gimelshein, Luca Antiga, et al. Pytorch: An imperative style, high-performance deep learning library. *Advances in neural information processing systems*, 32, 2019.
- [37] Matthias Fey and Jan Eric Lenssen. Fast graph representation learning with pytorch geometric. *arXiv preprint arXiv:1903.02428*, 2019.

A Properties of MDP Formulation

Although relevant DRL algorithms proposed before have reached competitive performance, they all neglect the value of waiting and arrange ope-ma pairs as soon as possible, which makes them impossible to reach optimality in some cases. Initially, we present a straightforward example to demonstrate this and subsequently show that our formulation is equivalent to the original IPPS problem.

A.1 Example

There’s a simple example (FJSP or IPPS) explaining why the policy without waiting may miss the (near) optimal solution.

	ma1	ma2
ope1	1	1
ope2	3	1
ope3	4	2

In this problem, we have only 2 jobs, 2 machines and 3 operations. Operations for job 1 and 2 is {ope1, ope2} and {ope3} respectively and their processing times are above. The optimal schedule for this problem is {(ope1,ma1),(ope3,ma2),(ope2,ma2)}, which has a waiting decision and makespan of 3. However, in the policy without waiting, we would arrange an ope-ma pairly if there exists feasible pairs. Hence, the algorithm would process ope1 and ope3 at $t = 0$ and job1 would be available again at $t = 1$. Due to the loss of waiting and ope3’s long processing times, ope2 would be arranged to the same machine as ope1, which means that each job can only be processed on a single machine. Because the total processing times of two jobs on ma1 are both 4, the best makespan under algorithm without waiting would be 4 and cannot reach the optimality.

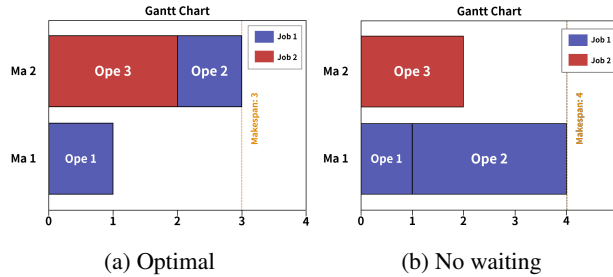


Figure 8

A.2 Proof of Theorem 1 (Equivalence)

Here we prove that our MDP is equivalent to the original IPPS problem. We define an IPPS solution as $D = \{d, s, e\}$, where $d = \{d_i | i = 1, 2, \dots, |d|\}$ is the set of schedules, with d_i being the i -th schedule allocating operation O_i belonging to J_i to machine M_i . The functions $s(d_i)$ and $e(d_i)$ represent the start and end times of d_i , and the makespan $M = \max\{e(d_i) | d_i \in d\}$. We can assume $s(d_i)$ are non-decreasing with i .

Recall: A schedule $d_i = (O_i, M_i, J_i)$ is eligible \iff all prerequisite operations of operation O_i have been finished, all operations that belong to job J_i and are not prerequisite for O_i hasn’t been scheduled and machine M_i and job J_i

are idle, which is equivalent to:

$$\begin{aligned} \forall O_m \in \mathcal{P}(O_i) \exists d_j \text{ s.t. } O_j \in d_i \ \& \ e(d_j) \leq s(d_i) \\ \forall O_m \in \mathcal{A}(O_i) \forall d_j \in \{d_p | s(d_p) \leq s(d_i)\}, O_m \neq d_j \\ e(d_t) \leq s(d_i), \forall d_t \text{ s.t. } M_i = M_t, t \leq i \\ e(d_t) \leq s(d_i), \forall d_t \text{ s.t. } J_i = J_t, t \leq i \end{aligned}$$

where $\mathcal{P}(O_i)$ is the set of prerequisite operations of operation O_i , and $\mathcal{A}(O_i)$ is the set of operations belong to same job with O_i and not in $\mathcal{P}(O_i)$. For convenient discussion, we define $\mathcal{R}_i = \{(O_h, M_h, J_h) | O_h = O_i \vee M_h = M_i\}$ for $d_i = (O_i, M_i, J_i)$ as the set of schedules containing prerequisite operations of O_i, M_i and J_i and the condition above will be:

$$\forall O_m \in \mathcal{P}(O_h) \exists d_j \in \mathcal{R}_i \text{ s.t. } O_m = O_j \quad (1)$$

$$e(d_t) \leq s(d_i), \forall d_t \in \mathcal{R}_i \quad (2)$$

$$\forall O_m \in \mathcal{A}(O_h) \forall d_j \in \{d_p | s(d_p) \leq s(d_i)\}, O_m \neq O_j \quad (3)$$

Lemma 1: for \forall IPPS solution D with makespan M , $\exists D'$ with makespan M' that satisfies:

$$\forall i \exists j \text{ s.t. } s(d_i) = e(d_j) \quad (4)$$

$$M' \leq M \quad (5)$$

Proof: Consider an IPPS solution D that does not satisfy (4). Assume d_i is the first schedule that $\nexists! j \text{ s.t. } s(d_i) = e(d_j)$. Notice that all schedules in a solution are eligible, we have:

$$\forall d_j \in \mathcal{R}_i, e(d_j) < s(d_i)$$

We create D' from D by following rule:

- $d' = d$
- $s'(d'_i) = \min\{e(d_j) | d_j \in \mathcal{R}_i\} < s(d_i)$
- $e'(d'_i) = s(d'_i) + \text{processing time of } d_i < e(d_i)$
- $s'(d'_t) = s(d_t), e'(d'_t) = e(d_t), \forall t \neq i$

Then, D' is also a solution because all schedules also satisfy (1) and (2) and d'_i satisfies (4). (1) holds because $d' = d$. And the reason that (2)(3) holds for all schedules in D' is:

- From our construction, d'_i satisfies (2).
- d'_i satisfies (3), because

$$\{d_p | s'(d_p) \leq s'(d_i)\} \subseteq \{d_p | s(d_p) \leq s(d_i)\}$$
- For $t \neq i$, d'_t satisfies (2) because:
 - if $\forall j \ d'_j \in \mathcal{R}_t, e'(d'_j) \leq e(d_j) \leq s(d_t) = s'(d'_t)$
 - else, $e'(d'_j) = e(d_j) \leq s(d_t) = s'(d'_t)$
- For $t \neq i$, d'_t satisfies (3) because (assume the operation in d'_i, d'_t are O_m, O_n respectively):
 - if $O_m \notin \mathcal{A}(O_n)$, (3) holds as everything doesn't change.
 - else, we only need consider d_i as:

$$d'_j = d_j, s'(d'_j) = s(d_j), e'(d'_j) = e(d_j), j \neq i$$

we know $s(d_t) < s(d_i)$ from (3) and $d_t \in \mathcal{R}_i$, which means

$$s'(d'_t) < e'(d'_t) \leq s'(d'_i)$$

So, (3) holds

Also, as $e'(d'_j) \leq e(d_j), \forall j, M' \leq M$. Keep following the procedure described above, we can find a solution \hat{D} satisfies (4)(5).

Lemma 2: For any solution D satisfying (4), it can be attained by MDP.

Proof: In our MDP formulation described before, a schedule $d_i = (O_i, M_i, J_i)$ is eligible in the time step t if (1) (2) (3) holds when $s(d_i) = t$, so we need to prove that all $s(d_i)$ can be attained in MDP. Notice that the support set of $\{s(d_j) | d_j \in D\}$ can be written as a non-decreasing sequence $0 = s_0, s_1, \dots, s_N$. We prove by induction:

(1) Basic case, start time 0 can be attained by MDP and MDP can schedule as same as D for d_i with $s(d_i) = 0$, which is obvious.

(2) Assume $\forall s_i \in \{s_t | s_t \leq s_k, k < N\}$ can be attained by MDP, and MDP have same schedules with start time $\leq s_k$ with original solution D . Notice We must has a completion time that equals s_{k+1} as all schedules with start time $\leq s_k$ is as same as D and we can keep waiting until time equals s_{k+1} because each time-step is a completion time. Then from (4), we can know s_{k+1} can be attained and MDP have same schedules with start time $\leq s_k + 1$ with original solution D .

A trajectory given from MDP must be a feasible solution because the action space design guarantee (1)(2)(3) must hold. Also, from Lemma 1 and Lemma 2, we know that for any optimal solution in original problem, we can get another optimal solution that can be given by MDP by a simple adjustment. So, it's equivalent to optimize original problem and MDP formulation problem.

B Graph Features

Raw features for Nodes:

- Operations:
 - Number of prerequisite operations.
 - Whether this operation is scheduled.
 - Whether operation is feasible.
 - Waiting time for a feasible operation(=0 for infeasible operations).
 - Time remained for the processing operation that is scheduled(=0 for unscheduled operation).
- Machines:
 - Number of neighboring operations.
 - The time when this machine becomes idle.
 - Utilization: ratio of the non-idle time to the total production time.
 - Whether the machine is working.
 - Idle time from available time to now.
 - Time remained for working machine to finish the working operation.
- Combinations:
 - Estimated completion time for these combinations.
 - Ratio of estimated end time to estimated min end time for combinations associated to the same job.
- Jobs:
 - Ratio of estimated end time to max estimated end time for all jobs.

Raw features for edges:

- Operations \Leftrightarrow Machines:
 - Processing time used by the machine to process the operation.

C MILP Model

To attain the optimal solution, we implement the MILP (Mixed Integer Linear Programming) model suggested by[12] using the CP-SAT solver of OR-Tools, an open source optimization library developed by Google. For more details, please refer cited paper.

Signal:

- i, i' : Job indices, $1 \leq i \leq |n|$
- j, j' : Operation indices, $1 \leq j \leq |n_i|$
- k, k' : Machine indices
- h : Combination index
- O_{ij} : The j th operation of the i th job
- O_{ihj} : The j th operation of the h th combination of the i th job

Sets and Parameters:

- A : A very large positive number.
- P_{ijk} : Processing time of job O_{ij} on machine k .
- R_h : The set of jobs contained in the h th combination of job i .
- K_i : The set of all combinations of job i .
- n : The set of jobs.
- n_i : The set of all jobs in the network diagram of job i .
- M_{ij} : The set of all candidate machines for job O_{ij} .
- $Q_{ijj'}$: Equals 1 if job O_{ij} is processed ly or directly before job $O_{ij'}$; equals 0 otherwise.

Variables:

- X_{ihjk} : Equals 1, if Operation O_{ihj} is allocated to Machine k .
- C_{ihj} : The completion time of the operation O_{ihj} .
- C_{\max} : Maximum makespan.
- Y_{ih} : Equals 1 if the h th combination of job i is selected; equals 0 otherwise.
- $Z_{ijj'}$: Equals 1 if job O_{ij} is processed directly or indirectly before job $O_{ij'}$; equals 0 otherwise.

Constraints:

For each job i , exactly one combination h must be selected.

$$\sum_{h \in K_i} Y_{ih} = 1, \quad \forall i$$

If combination h for job i is selected, the sum of operations in the combination is equal to 1, else it equals 0.

$$\sum_{k \in \mathcal{M}_{ij}} X_{ihjk} = Y_{ih}, \quad \forall i, h \in K_i, j \in R_{ih}$$

If combination h is not selected, the completion time of all operations in the combination is 0.

$$A \cdot Y_{ih} \geq C_{ihj}, \quad \forall i, h \in K_i, j \in R_{ih}$$

Guarantee correct completion time of operations.

$$C_{ihj'} \geq C_{ihj} + \sum_{k' \in M_{y'}} X_{ihj'k'} P_{ij'k'},$$

$$\forall i, h \in K_i, j, j' \in R_{ih}, j \neq j', V_{ij'} = 1$$

$$Z_{ijj'} + Z_{ij'j} = 1, \quad \forall i, j, j' \in n_i, Q_{ijj'} + Q_{ij'j} = 0, j \neq j'$$

$$C_{ihj'} \geq C_{ihj} + \sum_{k' \in M_v} X_{ihj'k'} P_{ij'k'} - A(1 - Z_{ijj'}),$$

$$\forall i, h \in K_i, j, j' \in R_{ih}, j \neq j'$$

Guarantee the processing order of operations in the same machines.

$$C_{ih'j'} \geq C_{ihj} + X_{i'h'j'k'} P_{i'k'}$$

$$- A(1 - W_{ijj'j'}) - A(2 - X_{ihjk} - X_{i'h'j'k'}),$$

$$C_{ihj} \geq C_{ih'j'} + X_{ihjk} P_{ijk} - A \cdot W_{ijj'j'}$$

$$- A(2 - X_{ihjk} - X_{ih'j'k'}),$$

$$\forall i, i', i \neq i', h \in K_i, h' \in K_{i'}, j \in R_{ih},$$

$$j' \in R_{i'h'}, k, k' \in M_{ij} \cap M_{ij'}, k = k'$$

Makespan is the maximum completion time of all operations.

$$C_{\max} \geq C_{ihj}, \quad \forall i, h \in K_i, j \in R_{ih}$$

D Problem Generation Approach

Based on the structure of AND/OR graph, we generate jobs by computing direct acyclic graphs and add OR-paths recursively. After assigning machines and corresponding processing time to each operation under a certain distribution, we randomly combine jobs for various IPPS problems.

Here, we define OR-link path as the sub-path, a path that is not the OR-link path as the main-path.

D.1 Non-Conforming Situations

In the following 2 scenarios, there are links between sub-paths and main-path such that the order of operation cannot be determined by definition.

- **Link from main-path to sub-path:** It is unclear whether operation 12 can be executed as it must be completed after operation 7 and 11 while operation 12 is in an OR-link path (as shown in Figure 9a).
- **Link from sub-path to main-path:** It's unclear that operation 12 can be done when operation 6 is not completed. (as shown in Figure 9b).

To avoid the scenarios above where operations in the main path and sub-path are linked, we employ a nested approach to generate the problem incrementally. The specific steps are as follows.

Well-Defined IPPS Problems Generation

Step 1: Construct Directed Acyclic Graph (DAG) as Main-path

- Input: Range of the number of operations in main-path, Maximum Out-degree...
- Initialize the start node and end node, then establish a sequence of operation nodes between the start and end nodes under input requirements.

Step 2: Add Sub-path to Main-path

- Input: The number of OR-connector, range of the number of total operations and operations in each sub-path, Maximum number of OR-connector's out-degree
- Randomly select n edges from the main path as initiation and integration points for the OR sub-paths, then generate m_i sub-paths with k_i nodes between originally chosen edge i . n, m, k is randomly decided under input requirements.
- For each added OR-path, randomly add and-path into it by selecting edges in sub-paths then generate and-path between the chosen edge.

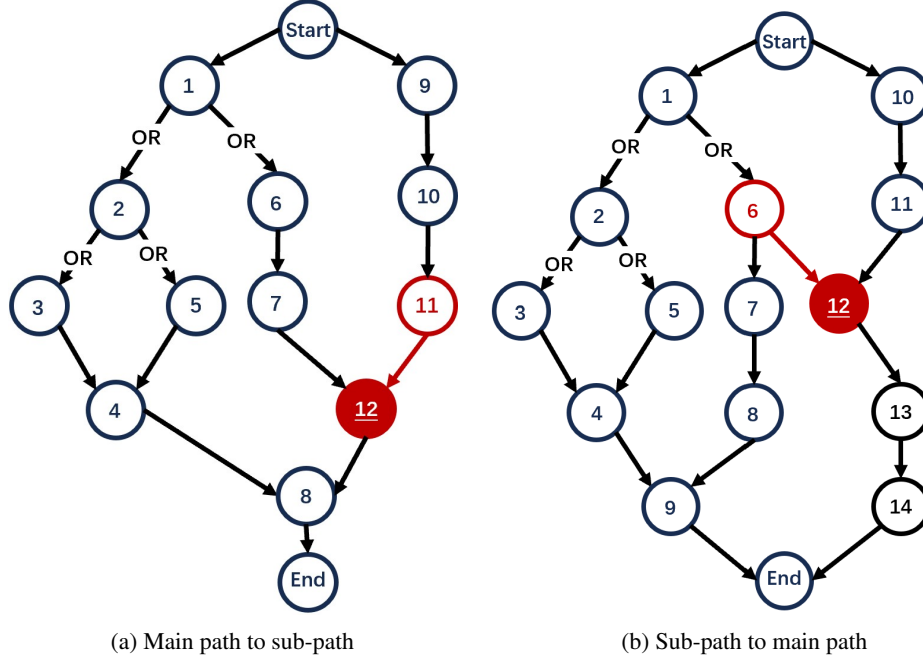


Figure 9: Comparison of path transitions.

- Every time insert paths to a chosen edges, if an edge of a join-node (where two sub-path emerge) is chosen, we automatically create a supernode at the end of the new sub-path, which then connects to the original join node.
- Check if the number of total operations meets the constraint. If not, generate a new job. Otherwise, save the well-defined job.

Step 3: Assignment of Machine and Processing Time

- Input: The number of machines, the range of processing time and the probability that one machine is assigned to each operation.
- For each operation, randomly assign machines to the operation using input probabilities with processing time uniformly generated by range of processing time.

Step 4: Combine Jobs to a Well-defined Problem

- Input: The number of jobs and machines
- Randomly combine required jobs number of well-defined jobs using the required number of machines.

E Infrastructure and Configuration

E.1 Infrastructure

We use a machine with an 11th Gen Intel(R) Core(TM) i7-11800H @ 2.30GHz CPU and NVIDIA GeForce RTX 3070 GPU for DRL and greedy dispatching rules. For solving MILP by OR-tools CP-SAT Solver, we use 32 cores of an Intel Xeon Platinum 8469C at 2.60 GHz CPU with 512 GB RAM. Our core functions are implemented using PyTorch[36] and PyTorch Geometric(PyG)[37].

E.2 Neural Networks Parameters

Below are the essential settings for our neural networks. Note that the length of lists in the Value column for hidden_dims or num_heads indicates the depth.

Parameter	Value
actor hidden_dims (layers)	[64, 32]
critic hidden_dims (layers)	[64, 32]
GNN pooling_method	mean
GNN jumping_knowledge	max
GNN model	GAT
GNN num_heads (layers)	[2, 2, 2]
GNN hidden_dim	64

E.3 Environment Parameters

We run 3 instances in a batch parallel and the size of validation set is set to 20.

Parameter	Value
batch_size	3
valid_batch_size	20

E.4 Training Parameters

Below are the training configurations. The learning rate (lr) and betas are fundamental parameters of the Adam optimizer. The parameter eps_clip in PPO-clip is adjusted by adding a multiplier (clip_multi) and an upper bound (clip_ub) to increase it to the upper bound. It’s important to note that lr, gamma, and parallel_iter(interval of changing instances) were tuned, and we identified a range that yielded competitive results in our tuning experiment. In our final trained model, we selected values of 5e-4, 0.99, and 20 respectively.

Parameter	Value
lr	5e-5 - 5e-4
betas	[0.9, 0.999]
gamma (Discounting rewards)	0.95 - 0.995
A_coeff (weight of policy loss)	1
clip_ub	0.5
K_epochs (update epoch in PPO)	3
eps_clip	0.3
vf_coeff (weight of value loss)	0.5
clip_multi	1.002
entro_coeff (weight of entropy loss)	0.05
parallel_iter	20 - 50
save_timestep (validate interval)	10
max_iterations	30000
minibatch (update batchsize in PPO)	512
update_timestep (update interval)	5
entropy_discount	0.997

F More Experiment Results

F.1 Ablation Experiments

To demonstrate the effectiveness of our reward function design along with the heterogeneous graph and updating design, we perform two ablation experiments using datasets with (5 jobs, 3 machines) as described previously. In these ablation experiments, all curves maintain the same configurations and run for 1500 training epochs, and we assess the validation curve (per 10 epochs).

Figure10a presents a comparison between the Naive Reward, which utilizes the difference in the maximum finished time of the scheduled operations, and our estimation-based Reward. Our reward function shows improved stability and competitiveness.

Figure10b presents a comparison of three distinct graph-based state representations: the **O-M graph**, which utilizes a graph with only two types of nodes — operation and machine, the **Not-residual graph** that retains nodes which are

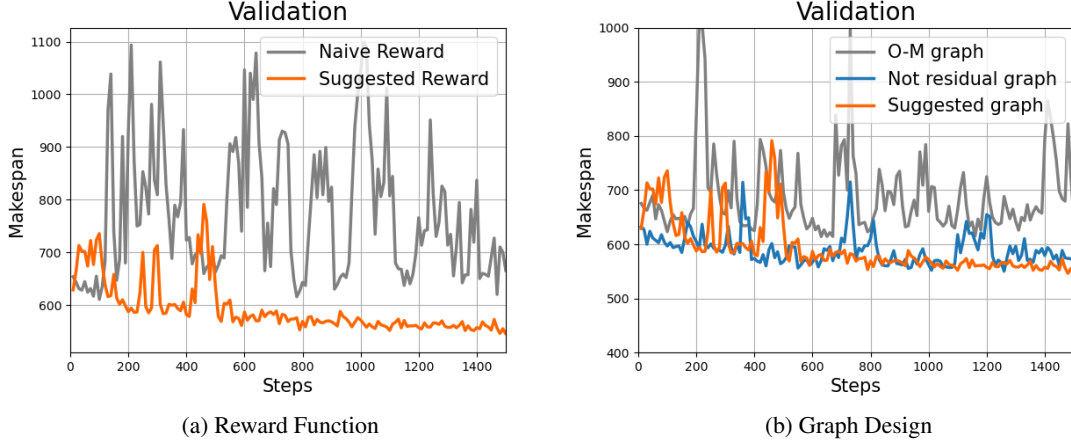


Figure 10: Comparison of path transitions.

ineligible or unnecessary, and our proposed graph with four types of nodes, which exclusively keeps eligible nodes as previously detailed. The proposed graph shows enhanced competitiveness and stability. Furthermore, it achieves a faster inference speed than the **Not-residual graph** due to the reduced aggregation of neighborhood information.

F.2 Additional Experiment in Large-scale Problem

As shown in Table 4, the difference between the results of DRL and Greedy decreases as the size of the problem increases, indicating that our methods are particularly effective for large-scale problems. We present experimental results from two relatively large, generated datasets: 16×20 and 20×25 in the main text. To further assess our efficiency, we conduct an additional experiment on 10 instances, each with 25 jobs and 20 machines. The results, shown in Table 7, further confirm that our method has significant potential for large-scale problem solving.

G Details of Greedy Dispatching Rules

G.1 Selecting Operation Rules

We utilize established greedy rules for FJSP within IPPS. To implement these FJSP rules, we initially choose a single combination for each job before application, as the rule is only executable with one specific combination.

In addition, we use a greedy rule designed for IPPS suggested by [35], which we call Muhammad.

- **First In First Out (FIFO)**, which handles the earliest operation in a machine’s queue to be processed.
- **Most Work Remaining (MWKR)**, which handles the job that has the largest amount of work left to be done.
- **Most Operation Number Remaining (MOR)**, which handles the job with the greatest number of remaining tasks.
- **Muhammad**, which selects a job according to the following probability:

$$P_i = \frac{C_i}{\sum_i C_i}$$

where C_i is determined based on the ratio of the estimated finish time of the job T_m to the critical time T_c . The definitions of T_m and T_c are as follows:

T_m refers to the minimum machining time calculated by summing the shortest processing times for all operations in a job, and the job with the largest T_m is identified as the critical job, with its machining time defined as the critical time T_c .

The values of C_i are then assigned according to the following conditions:

Condition	C
$T_m \geq 0.95T_c$	5
$0.85T_c \leq T_m < 0.95T_c$	4
$0.70T_c \leq T_m < 0.85T_c$	3
$0.50T_c \leq T_m < 0.70T_c$	2
$T_m < 0.5T_c$	1

To assign priorities, each job’s machining time T_m is compared with T_c , and a critical value C_i is assigned based on the conditions outlined in the table.

G.2 Selecting Machine Rules

For the machine selection criteria, the following rules have been considered:

- **Shortest Processing Time (SPT)**, which assigns a machine with the shortest processing time for an operation.
- **Earliest Ending Time (EET)**, which selects the machine where an operation can start earliest.
- **Least Utilized Machine (LUM)**, which selects the machine with least load.

G.3 Workflow

The Algorithm 1 displays the workflow of greedy rules. Each time an O-M pair is selected, we assign its start time to the earliest possible moment it can begin processing.

Algorithm 1 Greedy Dispatching Rules

Require: Repeat times \mathcal{N} .

- 1: Loading instances and Initializing environment
- 2: **for** $n = 1, 2, \dots, \mathcal{N}$ **do**
- 3: **while** s_t is not terminal **do**
- 4: Use Greedy Rules to select a O-M pair.
- 5: Schedule the pair at the earliest possible time.
- 6: Receive reward r_t and enter the next state s_{t+1} .
- 7: Update environment.
- 8: **end while**
- 9: **end for**
- 10: Choose the solution with min makespan.
- 11: **return**

H Experiment Details in Open Benchmarks

H.1 Algorithms

In this section, we present a detailed training and testing process.

H.1.1 Training Phase

For training, we use the PPO-clip algorithm. The pseudo-code of PPO algorithm is as follows.

H.1.2 Inference Phase

DRL-Sample (DRL-S) and DRL-Greedy (DRL-G) are two methods used during the inference phase. Specifically, DRL-G selects actions based on the highest probability, whereas DRL-S selects actions according to the probability distribution determined by the actor. The pseudo-code of these methods are as follows:

H.2 Results

The complete results of the Kim dataset are shown in Table 5 and Table 6.

Algorithm 2 Training procedure of PPO-clip

Require: Total training epoch is \mathcal{T} , the interval of changing instances is \mathcal{P} and the interval of updating is \mathcal{U}

- 1: Initializing trainable parameters ω of HGAT, policy network **Actor** $_{\theta}$ and Value **Critic** $_{\phi}$ network.
 - 2: Initializing Data-Generator or preparing set of IPPS instances.
 - 3: **for** iter = 1, 2, ..., \mathcal{T} **do**
 - 4: Loading data to a batch and Initializing environment
 - 5: **for** $b = 1, 2, \dots, \mathcal{P}$ **do**
 - 6: **while** s_t is not terminal **do**
 - 7: Extract embeddings of O-M pairs.
 - 8: Sample $a_t \sim \mathbf{Actor}_{\theta}(\cdot|s_t)$
 - 9: Receive reward r_t and enter next state s_{t+1}
 - 10: Update environment and memory.
 - 11: **end while**
 - 12: **if** $b \bmod \mathcal{U} = 0$ **then**
 - 13: Flatten states in memory.
 - 14: Calculate PPO loss.
 - 15: Update network parameters.
 - 16: **end if**
 - 17: **end for**
 - 18: **end for**
 - 19: **return**
-

Algorithm 3 DRL-G

Require: Repeat times \mathcal{N} .

- 1: Load the models that have already been trained.
 - 2: Loading instances and Initializing environment
 - 3: **for** $n = 1, 2, \dots, \mathcal{N}$ **do**
 - 4: **while** s_t is not terminal **do**
 - 5: Extract embeddings of O-M pairs.
 - 6: Select $a_t = \mathbf{argmax}(\mathbf{Actor}_{\theta}(\cdot|s_t))$
 - 7: Get the next state s_{t+1}
 - 8: Update environment.
 - 9: **end while**
 - 10: **end for**
 - 11: Choose the solution with min makespan.
 - 12: **return**
-

Algorithm 4 DRL-S

Require: Repeat times \mathcal{N} .

- 1: Load the models that have already been trained.
 - 2: Loading instances and Initializing environment
 - 3: **for** $n = 1, 2, \dots, \mathcal{N}$ **do**
 - 4: **while** s_t is not terminal **do**
 - 5: Extract embeddings of O-M pairs.
 - 6: Sample $a_t \sim \mathbf{Actor}_{\theta}(\cdot|s_t)$
 - 7: Get next state s_{t+1}
 - 8: Update environment.
 - 9: **end while**
 - 10: **end for**
 - 11: Choose the solution with min makespan.
 - 12: **return**
-

Size	DRL-G			DRL-S		
	4×5	5×3	6×5	4×5	5×3	6×5
6×15	6.04%	7.23%	7.19%	0.13%	-0.18%	0.63%
9×15	-0.08%	2.17%	-1.05%	-6.25%	-5.75%	-6.29%
12×15	-1.84%	0.09%	-3.60%	-9.80%	-10.15%	-10.70%
15×15	-6.29%	-9.19%	-5.79%	-14.62%	-12.80%	-14.42%
18×15	-10.71%	-4.54%	-6.72%	-10.16%	-10.34%	-11.07%

Table 4: Average Gap Across Different Problem Sizes in the Kim dataset. The gap is relative to the best greedy rule for each problem.

Greedy rules	MWKR			MOR			FIFO			Muhammad			BCI
	SPT	EFT	LUM	SPT	EFT	LUM	SPT	EFT	LUM	SPT	EFT	LUM	
problem01	452	523	543	427	532	518	475	544	538	427	472	494	427
problem02	422	475	460	387	392	393	438	435	431	398	376	387	376
problem03	417	473	447	385	422	420	469	491	504	374	388	378	374
problem04	369	381	359	319	329	331	382	361	371	311	330	336	311
problem05	419	555	455	386	388	392	423	388	414	375	364	369	364
problem06	571	537	509	558	508	491	504	536	572	526	505	489	489
problem07	447	500	571	434	401	434	443	456	483	425	392	388	388
problem08	536	448	429	432	393	401	443	403	414	427	378	395	378
problem09	494	523	505	544	511	535	427	533	518	429	486	474	427
problem10	540	537	521	492	510	489	567	553	564	505	506	509	489
problem11	536	513	495	463	420	433	502	470	521	447	442	446	420
problem12	446	477	465	402	353	399	505	398	445	391	377	400	353
problem13	653	610	596	563	500	503	641	566	618	564	521	503	500
problem14	555	614	617	517	441	487	496	521	540	500	456	461	441
problem15	494	571	505	555	499	511	490	514	537	483	496	485	483
problem16	581	583	586	533	490	507	601	585	627	570	529	547	490
problem17	614	618	551	543	452	490	551	547	517	540	518	517	452
problem18	503	533	512	488	391	429	524	476	476	454	445	457	391
problem19	677	663	654	604	513	540	655	606	637	596	559	566	513
problem20	618	590	571	539	475	488	579	552	571	577	532	543	475
problem21	662	669	621	614	508	512	565	574	648	563	506	538	506
problem22	709	721	718	673	535	557	640	622	693	630	587	601	535
problem23	642	662	628	579	487	517	621	639	641	562	566	570	487
problem24	770	756	740	709	551	607	754	714	716	696	636	648	551
Average	546.95	563.83	544.08	506.08	458.38	474.33	528.96	520.17	541.50	490.47	473.63	479.21	458.38

Table 5: Greedy Result for Kim.

In Table 4, we compare the gap relative to the best greedy result for each problem across different sizes. It is evident that the gap between the results of DRL and Greedy decreases as the problem size increases. This suggests that our method demonstrates significant potential in solving large-scale problems.

Problem	DRL-G			DRL-S			Greedy		OR-tool	LB*
	4×5	5×3	6×5	4×5	5×3	6×5	Best One†	Best Choice‡		
problem01	523	496	486	462	468	484	532	427	427	427
problem02	377	413	421	360	363	364	392	376	343	343
problem03	372	375	390	372	363	367	422	374	346	344
problem04	334	364	325	318	312	315	329	311	306	306
problem05	343	338	345	332	330	331	388	364	318	318
problem06	528	496	533	483	474	487	508	489	427	427
problem07	396	403	392	374	383	385	401	388	372	372
problem08	397	407	404	362	360	356	393	378	343	343
problem09	493	495	506	484	484	479	511	427	427	427
problem10	517	544	500	474	486	474	510	489	427	427
problem11	371	441	404	367	367	368	420	420	344	344
problem12	357	338	367	338	334	332	353	353	318	318
problem13	525	498	492	478	479	485	500	500	427	427
problem14	407	429	405	383	385	384	441	441	372	372
problem15	517	503	488	483	488	481	499	483	427	427
problem16	510	518	505	483	478	475	490	490	427	427
problem17	392	419	405	377	372	373	452	452	382	344
problem18	411	390	385	350	353	344	391	391	322	318
problem19	504	557	502	472	473	477	513	513	427	427
problem20	439	424	434	399	389	387	475	475	385	372
problem21	518	529	496	474	480	475	508	506	427	427
problem22	538	496	506	473	487	473	535	535	427	427
problem23	423	433	457	401	406	403	487	487	534	372
problem24	492	526	514	495	494	490	551	551	455	427

Table 6: DRL Result For Kim. †Best One refers to the result of greedy rule that has a minimum average makespan while ‡Best Choice is the best greedy result for each problem. *LB refers to lower bound of Kim dataset demonstrated in [6]

Problem	DRL-S			DRL-G			Greedy		OR-tool
	4×5	5×3	6×5	4×5	5×3	6×5	Best One†	Best Choice‡	
problem01	412	424	415	427	446	438	480	480	621
problem02	417	412	423	424	438	781	473	473	1659
problem03	421	419	415	496	438	499	483	483	692
problem04	418	413	423	459	444	452	479	479	1045
problem05	417	421	419	537	420	434	480	480	1134
problem06	421	417	414	448	449	430	479	479	887
problem07	417	419	416	429	421	429	472	472	481
problem08	420	420	419	465	440	442	476	476	1152
problem09	422	419	418	438	432	452	465	465	884
problem10	419	410	425	445	439	455	473	473	469
Average Gap	-	-	-	-	-	-	-	-	-
	46.32%	46.43%	46.28%	41.82%	44.01%	40.46%	38.93%	38.93%	

Table 7: Performance in problems of size 25×20 . †Best One refers to the result of greedy rule that has a minimum average makespan while ‡Best Choice is the best greedy result for each problem.